12 October 2001

ELSEVIER

Chemical Physics Letters 346 (2001) 503–511

CHEMICAL PHYSICS LETTERS

www.elsevier.com/locate/cplett

Frequency and time-domain analysis of excited-state intramolecular proton transfer. Double-proton transfer in 2,5-bis(2-benzoxazolyl)-hydroquinone?

J. Weiß [a], V. May [a,*], N.P. Ernsting [b], V. Farztdinov [b], A. Mühlpfordt [b,1]

[a] *Institut für Physik, Hausvogteiplatz 5-7, Humboldt-Universität zu Berlin, D-10117 Berlin Germany*
[b] *Institut für Chemie, Bunsenstrasse 1, Humboldt-Universität zu Berlin, D-10117 Berlin Germany*

Received 19 March 2001; in final form 3 August 2001

Abstract

2,5-bis(2-benzoxazolyl)-hydroquinone has two reactive sites for excited-state intramolecular proton transfer (ESIPT) AH...B → A...HB. To carry out a frequency and time-domain analysis of the PT the reactive system is modeled in terms of diabatic educt and product potentials for each proton plus a single heavy atom coordinate per proton. The latter are assumed to modulate the proton motion which is treated in the adiabatic approximation. By dissipative propagation of this four-mode system, the structured absorption spectrum of the isolated molecule is simulated. Comparison with the observed vibronic spectra suggests the existence of a double-proton transferred state in the isolated molecule. This is confirmed by semiempirical quantum-chemical calculations.

1. Introduction

Hydrogen bonding is fundamental to chemical structure and reactivity. Multiple H-bonds explain the properties of water, they form the structural basis for the native folding pattern of proteins, and they hold together specific base pairs in the DNA building blocks of life [1]. Watson and Crick speculated already in their classical paper [2] how DNA replication might result in 'false' base pairs AC or TG: at the active site in the DNA polymerase, the tautomer A^{imino} might be used instead of G (or T^{enol} instead of A) which should then relax into the more favorable form. This idea spurred interest in systems with multiple internal hydrogen bonds and their tautomerisation reaction.

The reaction is best studied in the electronically excited state where it may be triggered by ultrafast optical excitation. This process (for reviews see [1,3,4]) is termed 'excited-state intramolecular proton transfer' (ESIPT) even though the charge distribution may change little during tautomerisation in which case the term 'H-transfer' would be more appropriate. Radiative damage to DNA, for example, was explained by tautomerisation in base pairs [5]. For such reactions involving two H-bonds, dimeric 7-aza-indole $(7AI)_2$ provides a prominent example (see [6] and references therein) and its mechanism was discussed intensely, i.e.,

* Corresponding author. Fax: +49-30-238-47-63.
E-mail address: may@physik.hu-berlin.de (V. May).
[1] Present address: Carl Zeiss, Lithography Optics Division, D-73446 Oberkochen, Germany.

0009-2614/01/$ - see front matter
PII: S0009-2614(01)00886-7

whether the process is sequential [7–9] or simultaneous (concerted) [10]. Many ESIPT systems have two outstanding features: (i) the electronic change proceeds on a femtosecond time scale [11–13] and (ii) the spectra [14–16] and dynamics [11–13] show strong activity in low-frequency modes which modulate the PT distance. This is why ESIPT involving two reactive sites AH...B → A...HB must be considered as the motion of a joint wavepacket for the two H atoms coupled to the skeletal motion of the corresponding donor and acceptor atoms.

Because of the fundamental character of PT the relevant literature is huge (an overview is given in [17,19,20]). However double PT has been analyzed less intensely and often without noting the specifics of two particles moving (see, e.g., [21]). Only recently the two-particle character of double PT has been emphasized. In [22] the quantum-mechanical motion of two protons was embedded into a molecular dynamics simulation for the heavy atoms while nonadiabatic transitions were treated by surface hopping. A semiclassical description of all degrees of freedom including both protons has been given in [20]. But if one wants to compute transient optical spectra (for example the differential absorption of a pump–probe experiment) this semiclassical approach requires many trajectories from which spectra must then be assembled.

The present Letter follows a different strategy which is oriented towards the computation of pump–probe spectra for comparison with experimental data. We use the density matrix method for the description of ultrafast PT because it provides direct and well-established access to optical data (for example [23]). Furthermore, irreversible dephasing and energy relaxation are treated in a manner which appears natural for large molecules or for molecules in the condensed phase. This approach will be demonstrated with the molecule 2,5-bis(2-benzoxazolyl)-hydroquinone (BBXHQ, Fig. 1) which has two phenolic –OH groups, each H-bonded to =N– of the adjacent benzoxazolyl moiety. This enol–enol tautomer (AA in Fig. 1) is the most stable form in the electronic ground state.

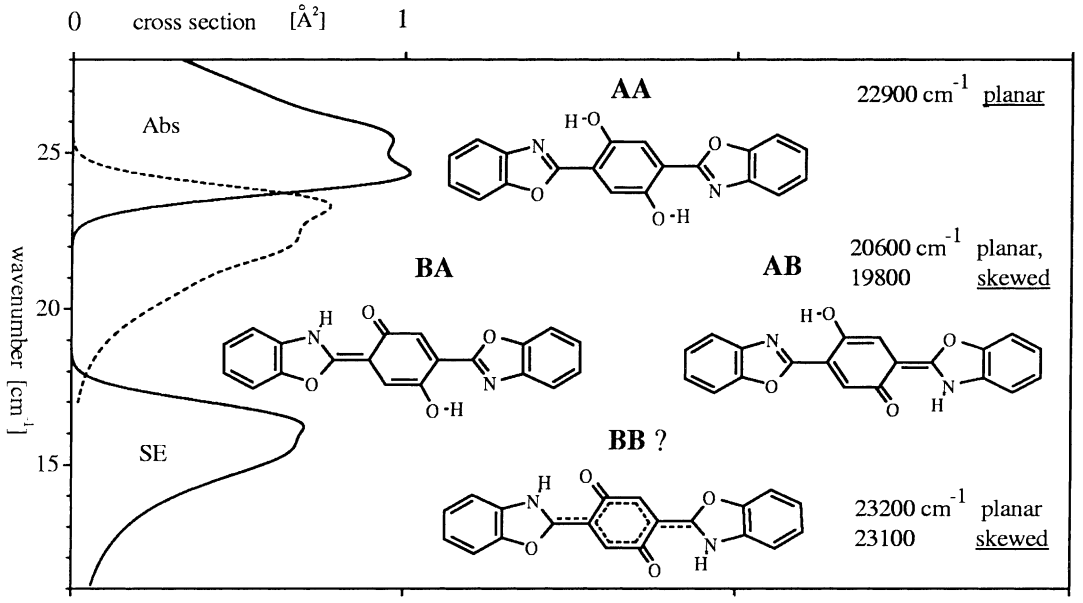

Fig. 1. Absorption (Abs) and stimulated emission spectra (SE, solid lines) of BBXHQ in tetrahydrofurane. After optical excitation the enol–enol form AA should show blue emission (dashed line) but instead transfers a H-atom to form the single keto forms BA or AB which emit in the red. Double PT leads to the keto–keto form BB which has not yet been observed. The potential energy of the S_1 tautomers from semiempirical calculations is given relative to S_0, with the locally stable form underlined.

Let us first consider BBXHQ in unpolar or weakly polar nonprotic solvents. Electronic $S_1 \leftarrow S_0$ ($\pi\pi^*$) excitation alters the charge distribution: the excited enol form AA is no longer stable so that its 'normal' blue fluorescence is much reduced; instead a labile hydrogen atom is transferred and two equivalent 'single keto' forms BA or AB (see Fig. 1) are created in the excited state within 110 fs [13]. Now keto fluorescence occurs in the red, as the electronic ground state has higher potential energy. The relative yield of blue and red fluorescence is a measure of the equilibrium $AA \leftrightarrow \{BA, AB\}$ in S_1 which in solvents is tilted towards the keto forms on the right. Essentially the same emission spectrum is observed when one OH-group is methylated; it was concluded that only single ESIPT takes place and that the 'double keto' form BB does not exist [24].

Next we turn to the isolated molecule which was studied in a supersonic jet by fluorescence [15] and photoelectron [25] spectroscopy. At low excess vibrational energies in S_1 one finds vibronic levels which fluoresce predominantly blue (and therefore have enol character) surrounded by levels which fluoresce red (hence have keto character). It was concluded that the enol and keto forms are nearly degenerate and that the rich level structure reflects their interaction which involves PT and skeletal motion.

Accidental degeneracy has been found in no other ESIPT compound so far, and the presence of two active sites opens the possibility of studying double PT $AA \rightarrow BA \rightarrow BB$. This is why BBXHQ provides a test case for modeling spectra and PT dynamics with the density matrix method. Here we begin by simulating the absorption line spectrum of the isolated molecule. The purpose is to establish a model Hamiltonian which may be extended for more detailed descriptions. Our simulations suggest the existence of a double-proton-transferred state in the isolated molecule which is confirmed by semiempirical quantum-chemical calculations.

2. Theoretical model and computational methods

In descriptions of single PT $AH \ldots B \rightarrow A \ldots HB$, the proton motion is commonly coupled to a collective heavy atom motion, i.e., a low-frequency skeletal eigenmode, which modulates the proton potential energy (see, e.g., [17,19]). The collective heavy atom motion strongly influences the skeletal separation $A \ldots B$, and the double-well potential for the H atom may be derived from diabatic enol and keto potential energy surfaces (PES). The proton frequencies are taken as independent from the skeletal displacement [17]. Since proton motion is considerably faster than the corresponding heavy atom motion, a second Born–Oppenheimer approximation can be applied and a nonadiabaticity operator describes the weak coupling between these fast and slow modes (for an overview and matrix elements see [18]). We adopt this approach for the present case of (possibly) double PT and hence use two sets of proton and heavy atom coordinates. Dissipation is accounted for by coupling the two heavy atom coordinates to a thermal reservoir of other intramolecular vibrations. The nuclear coordinates of our model are shown in Fig. 2. The proton coordinates x_m describe the position of the H atoms along their hydrogen bridge ($m = 1, 2$ can be identified with the left and right moiety, respectively) whereas the heavy atom coordinates R_m may be understood as collective skeleton coordinates

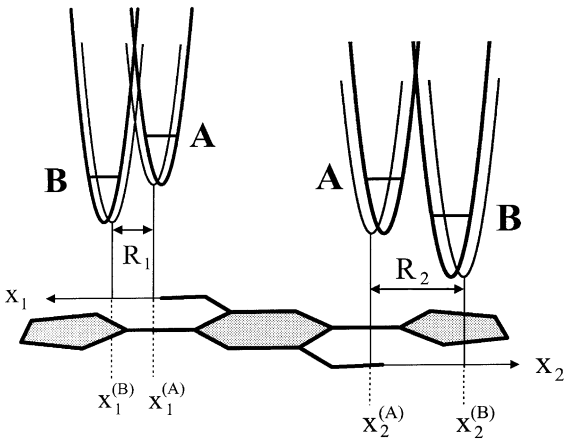

Fig. 2. Coordinates used for the construction of excited diabatic electronic states. Proton potential energy curves with nuclear scaffold in equilibrium for that configuration are indicated by thick solid lines. They are displaced (thin lines) by heavy atom motion.

which determine the proton equilibrium distance between the enol (A) and keto (B) forms. The bath of passive low-frequency coordinates is represented by the set $Z = \{Z_\xi\}$. Correspondingly, the total PES can be written as a sum of two terms, $U^{(\mathrm{S})}(x_1, x_2; R_1, R_2)$ and $U^{(\mathrm{S-R})}(R_1, R_2; Z)$. The first term governs the motion of the active system coordinates whereas the second term includes the coupling to the passive coordinates (system–reservoir coupling).

The system PES is discussed next. Note that single PT will disturb the C_{2h} symmetry of BBXHQ and the skeletal vibration may be different for the enol and keto forms in the S_1 state. For either tautomer, equilibrium values for R_1 and R_2 are obtained from quantum-chemical calculations (see below). A global ab initio PES on the other hand is prohibitively costly for large molecules and entails systematic errors with results of semiempirical methods, particularly when H bonding occurs [26]. Hence it is both convenient and more conducive to physical understanding to introduce model potentials and adopt them to experimental data. Here we use diabatic electronic states, each with an harmonic PES along the system nuclear coordinates, and an electronic coupling between them.

The diabatic excited states are described by electronic wavefunctions $\Phi_{\mathrm{ab}}(r)$ which correspond to the left hydrogen bridge in configuration a (= A or B) and the right one in configuration b. (We do not need concrete forms for these wavefunctions since all electronic matrix elements will be treated as parameters.) The PES for the excited diabatic state of configurations ab is denoted as

$$\begin{aligned} U^{(\mathrm{S})}_{\mathrm{ab}}(x_1, x_2; R_1, R_2) &= U^{(0)}_{\mathrm{ab}} + \frac{\mu_{\mathrm{pr}}\omega^2_{\mathrm{pr}}}{2}\left(x_1 - x_1^{(\mathrm{a})}\right)^2 \\ &\quad + \frac{\mu_{\mathrm{ha}}\omega^2_{\mathrm{ha}}}{2}\left(R_1 - R_1^{(\mathrm{a})}\right)^2 + \frac{\mu_{\mathrm{pr}}\omega^2_{\mathrm{pr}}}{2}\left(x_2 - x_2^{(\mathrm{b})}\right)^2 \\ &\quad + \frac{\mu_{\mathrm{ha}}\omega^2_{\mathrm{ha}}}{2}\left(R_2 - R_2^{(b)}\right)^2. \end{aligned} \tag{1}$$

Here the μ and ω represent oscillator effective masses and frequencies, and $x_m^{(\mathrm{a,b})}$ and $R_m^{(\mathrm{a,b})}$ give the equilibrium position of the proton (pr) and the heavy atom (ha) coordinates in moiety m and configuration a or b, respectively. The PES for the electronic ground state is denoted in a similar manner, but with ground-state reference energy $U_{\mathrm{g}}^{(0)}$ (set equal to zero in the following) and with a and b replaced by g. Table 1 gives a list of all relevant parameters. The equilibrium positions of the protons in Eq. (1) depend parametrically on the heavy atom coordinates. If R_m becomes smaller than its equilibrium value, then the barrier of the double-well potential has to decrease. A simple model for this behavior is obtained if one expands the proton equilibrium position $x_m^{(\mathrm{a})}$ in powers of $R_m - R_m^{(\mathrm{a})}$, yielding $x_m^{(\mathrm{a})}(R_m) \approx x_m^{(\mathrm{a})}(R_m^{(\mathrm{a})}) + k_m^{(\mathrm{a})}(R_m - R_m^{(\mathrm{a})})$. The correct behavior requires $k_m^{(\mathrm{A})} < 0$ and $k_m^{(\mathrm{B})} > 0$. In this way an indirect dependence of the proton PES on the R_m has been introduced. The coupling of the system to the reservoir modes (responsible for vibronic linewidths) is specified as follows. The reservoir modes are taken to be independent of the actual electronic state and couple to the heavy atom motion of the system via a simple bilinear coupling function. The reservoir modes themselves are treated within the framework of dissipative quantum dynamics and are characterized by a spectral density (see, e.g., [19]).

PT in the excited state is induced by electronic coupling matrix elements between the various enol and keto diabatic states. The expansion of the excited-state Hamiltonian reads (note $\hat{\mathrm{a}} = \mathrm{B}$ if $\mathrm{a} = \mathrm{A}$ and vice versa)

$$\begin{aligned} H_{\mathrm{e}} = \sum_{\mathrm{a,b,c,d}} \big\{ &\delta_{\mathrm{a,c}}\delta_{\mathrm{b,d}}(T_{\mathrm{nuc}} + U_{\mathrm{ab}}) \\ &+ (1 - \delta_{\mathrm{a,c}})\delta_{\mathrm{b,d}} V_{\mathrm{ab\hat{a}b}} + \delta_{\mathrm{a,c}}(1 - \delta_{\mathrm{b,d}}) V_{\mathrm{aba\hat{b}}} \\ &+ (1 - \delta_{\mathrm{a,c}})(1 - \delta_{\mathrm{b,d}}) W_{\mathrm{ab\hat{a}\hat{b}}} \big\} \times |\Phi_{\mathrm{ab}}\rangle\langle\Phi_{\mathrm{cd}}|. \end{aligned} \tag{2}$$

Table 1
Model parameters used to compute the spectrum of Fig. 2

$q^{(\mathrm{A})}$	0.1	$U_{\mathrm{g}}^{(0)}$	0 cm^{-1}
$q^{(\mathrm{B})}$	2.5	$U^{(0)}_{\mathrm{AA}} = U^{(0)}_{\mathrm{AB,BA}} = U^{(0)}_{\mathrm{BB}}$	23931 cm^{-1}
$Q^{(\mathrm{A})}$	1.3	V_{AB}	265 cm^{-1}
$Q^{(\mathrm{B})}$	1.5	W	1594 cm^{-1}
ω_{pr}	2700 cm^{-1}	$k_m^{(\mathrm{a})}$	0 cm^{-1}
ω_{ha}	114.7 cm^{-1}	γ	0.425 cm^{-1}

The dimensionless shifts in the PES relative to the ground state are defined as $q^{(\mathrm{a})}$ for the proton coordinates and $Q^{(\mathrm{a})}$ for the heavy atom coordinates. Their absolute values are given by $\sqrt{\omega_{\mathrm{pr}}\mu_{\mathrm{pr}}/2\hbar}x^{(\mathrm{a})}$ and $\sqrt{\omega_{\mathrm{ha}}\mu_{\mathrm{ha}}/2\hbar}R^{(\mathrm{a})}$, respectively. The quantities μ_{pr} and μ_{ha} denote the corresponding reduced masses.

This expression is the most general one based on the four excited diabatic states. Besides the diabatic Hamiltonian $T_{\rm nuc} + U_{\rm ab}$ with PES $U_{\rm ab} = U_{\rm ab}^{\rm (S)} + U_{\rm ab}^{\rm (S-R)}$ it includes various electronic coupling matrix elements. The elements $V_{\rm ab\hat{a}\hat{b}}$ and $V_{\rm aba\hat{b}}$ control the enol–keto coupling in the left and the right hydrogen bridge, respectively, whereas $W_{\rm ab\hat{a}\hat{b}}$ is a residual coupling between both hydrogen bridges. Note that the electronic couplings are not known but have to be determined by fitting the experimental spectra. For this reason it seems to be acceptable to reduce the electronic matrix elements $V_{\rm ab\hat{a}\hat{b}}$ and $V_{\rm aba\hat{b}}$ to a single one, $V_{\rm a\hat{a}}$, which equals $V_{\rm AB} \equiv V$ or $V_{\rm BA} \equiv V^*$. To achieve the correct splitting and oscillator strength of the spectral lines it may become necessary to take V real or complex. In the same manner we reduce the matrix elements $W_{\rm ab\hat{a}\hat{b}}$ (the two essentially different elements are $W_{\rm AABB}$ and $W_{\rm BAAB}$) to the single (but probably complex) quantity W.

Having fixed the diabatic electronic basis functions we will specify the nuclear wave functions for the proton and heavy atom motion by setting up the complete wave function of the active system. For the excited electronic state we have $\Psi_{\rm e} = \psi_{1{\rm a}\mu}(x_1;R_1)\psi_{2{\rm b}\nu}(x_2;R_2)\ \ \chi_{1{\rm a}M}(R_1)\chi_{2{\rm b}N}(R_2)\Phi_{\rm ab}$. The functions ψ for the two protons involve the quantum number μ (or ν) and the heavy atom functions χ are labeled by quantum number M (or N). It is appropriate to employ harmonic oscillator wave functions for all functions involved. A similar expression holds for the electronic ground state.

We are now ready to determine the absorption coefficient α at excitation frequency ω within a time-dependent formulation [27]. From the electronic ground state of BBXHQ with its enol–enol (AA) configuration only the excited diabatic state $\Phi_{\rm AA}$ is accessible. The dipole operator in the Condon approximation is therefore $\hat{\mu} = |\Phi_{\rm AA}\rangle\ \ d\langle\Phi_{\rm g}| + {\rm h.c.}$ with transition dipole moment d. The absorption coefficient can be written as $\alpha(\omega) = (4\pi\omega n_{\rm mol})/(\hbar c) I(\omega)$ where $n_{\rm mol}$ is the volume density of the molecules and $I(\omega)$ denotes the real part of the half-sided Fourier transform of the dipole–dipole correlation $C_{\rm d-d}^{(-)}(t)$. Because of the division of the molecular system into an active part and the remaining reservoir, a reduced statistical operator $\hat{\rho}(t)$ can be introduced which acts only in the state space of the active modes. Now we can write $C_{\rm d-d}^{(-)}(t) = {\rm tr_S}\{\hat{\mu}\hat{\sigma}(t)\}$ and the new quantity $\hat{\sigma}$ is propagated according to $\hat{\sigma}(t) = \exp(-{\rm i}\mathscr{L}_{\rm eff}t)[\hat{\mu}, \hat{\rho}_{\rm eq}]_-$. The superoperator $\mathscr{L}_{\rm eff}$ contains both, the dynamics in the active space, as well as the dissipative coupling to the bath-modes. In general, $\hat{\rho}_{\rm eq}$ incorporates thermal excitations of the heavy atom vibrations in the electronic ground state. For jet-cooled BBXHQ, however, we may assume that all vibrational modes are initially unexcited and set $T = 0$. With all these ingredients at hand the dipole–dipole correlation function is obtained as

$$C_{\rm d-d}^{(-)}(t) = |d|^2 \exp{\rm i}\left(\left(U_{\rm g}^{(0)}/\hbar + \omega_{\rm pr} + \omega_{\rm ha} + {\rm i}\gamma\right)t\right) \times \left\langle \psi_{1{\rm g}0}\psi_{2{\rm g}0}\chi_{1{\rm g}0}\chi_{2{\rm g}0}\Phi_{\rm AA} \mid \tilde{U}_{\rm e}(t) \mid \times \psi_{1{\rm g}0}\psi_{2{\rm g}0}\chi_{1{\rm g}0}\chi_{2{\rm g}0}\Phi_{\rm AA}\right\rangle, \quad (3)$$

where the dephasing rate γ originates from the system–bath coupling. The operator $\tilde{U}_{\rm e}(t)$ represents the time evolution in the excited electronic state and also accounts for dissipation. Transition amplitudes are introduced after inserting the complete set of excited state wave functions $\Psi_{\rm e}$ (note the incorporation of a time-dependent prefactor)

$$\mathscr{A}({\rm a}\mu, {\rm b}\nu, {\rm a}M, {\rm b}N; t) = \exp\left({\rm i}(U_{\rm AA}^{(0)}/\hbar + \omega_{\rm pr} + \omega_{\rm ha})t\right) \times \left\langle \psi_{1{\rm a}\mu}\psi_{2{\rm b}\nu}\chi_{1{\rm a}M}\chi_{2{\rm b}N}\Phi_{\rm AA} \mid \tilde{U}_{\rm e}(t) \mid \times \psi_{1{\rm g}0}\psi_{2{\rm g}0}\chi_{1{\rm g}0}\chi_{2{\rm g}0}\Phi_{\rm AA}\right\rangle. \quad (4)$$

These quantities, which depend on all four active degrees of freedom, are propagated in time. They determine the dipole–dipole correlation function, Eq. (3), which in turn gives the absorption coefficient α.

Finally, we compute the excited state wavepacket motion after an impulsive excitation using the transition amplitudes. If there is no dissipation, one obtains the double-proton probability distribution

$$P(x_1,x_2;t) = \langle \Psi(t)|x_1,x_2\rangle\langle x_1,x_2|\Psi(t)\rangle$$
$$= \sum_{\mathrm{a,b}} \sum_{M,N} \sum_{\mu,\nu,\lambda,\kappa} \psi^*_{\mathrm{a}\mu}(x_1)\psi_{\mathrm{a}\lambda}(x_1) \times \psi^*_{\mathrm{b}\nu}(x_2)\psi_{\mathrm{b}\kappa}(x_2) * \mathscr{A}^*(\mathrm{a}\mu,\mathrm{b}\nu,\mathrm{a}M,\mathrm{b}N;t) \times \mathscr{A}(\mathrm{a}\lambda,\mathrm{b}\kappa,\mathrm{a}M,\mathrm{b}N;t). \quad (5)$$

In the presence of dissipation Eq. (5) is still a good approximation of excited state dynamics if one includes a renormalization procedure to compensate for the decrease of the norm (see [27] for details).

3. Numerical results

The vibronic line spectrum of BBXHQ is shown in the upper panel of Fig. 3. Here the red fluorescence intensity is plotted as the excitation frequency is scanned up to 500 cm^{-1} of excess vibrational energy [28]. The transitions are readily sorted into clusters which form a progression in a 115 cm^{-1} mode, assigned to in-plane bending [29]. The cluster structure will now be explained for the first time, and we proceed to simulate the wavepacket dynamics of two-proton motion in the excited state.

The first cluster consists essentially of three vibronic bands and a very weak fourth one. Higher resolution of the central band reveals in fact two transitions of which one gives mainly blue and the other only red emission [29]. In the other clusters many more weak bands appear on a continuous background. The weak bands may originate from other low-frequency skeletal modes. In our treatment, weak bands and background around dominant vibronic lines are accounted for by broadening of the latter; the remainder of the continuous background is most likely due to spectral congestion. For the following we assume (i) that the experimental excitation spectrum in Fig. 3 resembles the absorption spectrum, (ii) that each cluster is essentially made up from four vibronic transitions arranged in three bands (the weaker fourth band is tentatively assigned to a hot transition, but see below), and (iii) that the contributing enol and keto forms are electronically degenerate on a low-frequency energy scale, say 100 cm^{-1}. As regards the high-frequency proton motion in S_1 only the vibrational ground state for the enol and keto forms need be considered because of the limited energy range. Activity in an OH stretching mode is not observed [15]; it follows that there is no significant displacement along that mode upon $S_1 \leftarrow S_0$ $(\pi\pi^*)$ excitation.

Simulations of the spectrum are intended to explore the model Hamiltonian for the excited state, Eq. (2). In this Letter we investigate the simplest scenario regarding (iii) above, i.e., all excited diabatic states (ab configurations) have the same electronic energy. A calculated spectrum is displayed in the lower panel of Fig. 3 and the corresponding parameters are collected in Table 1. The three dominant lines of each cluster are derived from the diabatic electron/proton states: the original enol–enol configuration $|\psi_{\mathrm{A}\mu=0}\psi_{\mathrm{A}\mu=0}\Phi_{\mathrm{AA}}\rangle$, the single-PT keto–enol configurations $|\psi_{\mathrm{B}\mu=0}$ $i_{\mathrm{A}\mu=0}\Phi_{\mathrm{BA}}\rangle$ and $|\psi_{\mathrm{A}\mu=0}\psi_{\mathrm{B}\mu=0}\Phi_{\mathrm{AB}}\rangle$, and the double-PT configuration keto–keto $|\psi_{\mathrm{B}\mu=0}\psi_{\mathrm{B}\mu=0}\Phi_{\mathrm{BB}}\rangle$. For real values of the enol–keto coupling V and the residual coupling W, the middle peak is doubly degenerate. Only one of the two has oscillator strength which leads to only three lines. Note that the same result is reached if the full C_{2h} symmetry, which is reflected in the Hamiltonian Eq. (2), is applied at the outset to construct symmetry-adapted diabatic states. From the regularity of the spectrum it can be inferred that the coupling between different triplets is weak compared to the coupling within each triplet, implying that the heavy atom configurations are almost identical in either enol or keto form. As a consequence the enol–keto coupling V as well as the residual coupling W are nearly diagonal with respect to heavy atom mode excitations. In our calculations the enol–keto coupling V causes a symmetric splitting into three lines and the residual coupling W is responsible for the asymmetry in the energy position. The fact that the peak at higher frequency within a triplet has more oscillator strength than the lowest one is due the fact that $(R^{(\mathrm{B})})$ is slightly greater than $(R^{(\mathrm{A})})$, see Table 1, in agreement with quantum-chemical calculations. Furthermore we

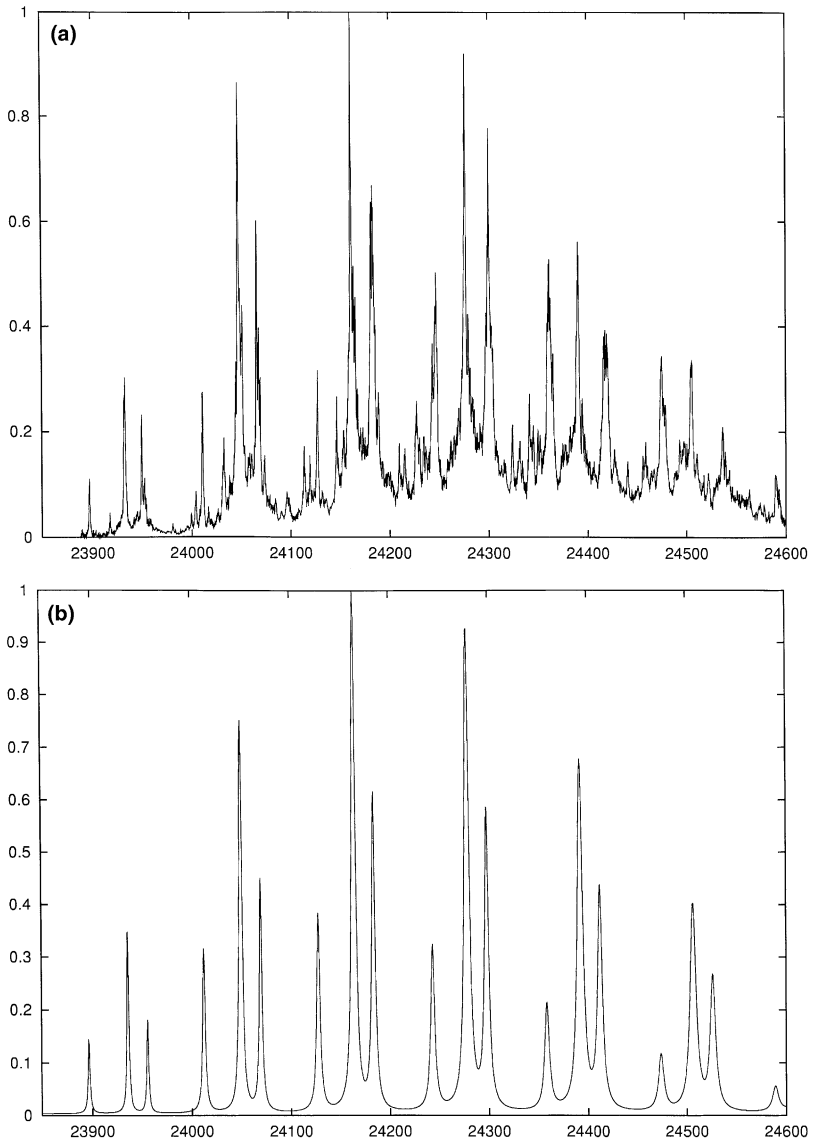

Fig. 3. Fluorescence excitation spectrum of isolated BBXHQ cooled in a supersonic jet [28] (a) and simulation by dissipative density matrix propagation (b).

find that any strong coupling between the proton states and heavy atom states which influences the PT dynamics (as controlled by the $k_m^{(A)}$ and $k_m^{(B)}$) at the same time destroys the regularity of the spectrum. This observation implies that the proton motion is only modestly influenced by the effective heavy atom vibration. After several test calculations we included two proton states and 10 heavy atom states for each site configuration and propagated the autocorrelation function up to 60 ps. This long propagation time is necessary because of the narrow linewidths of the peaks $\gamma = 8 \times 10^{-5}$ fs^{-1}, see Table 1.

The experimental spectrum in panel of Fig. 3 may also be interpreted as a four-fold splitting of degenerate lines. This can be achieved by choosing

a larger and now complex residual coupling W – with this choice the degeneracy of the middle peak is lifted and the hitherto dark transition is given oscillator strength. But this fourth line disappears, say for $M = 3$ quanta in the heavy atom mode, so that there is no clear pattern of four lines recognizable for all values of M. Therefore we found a splitting into a triplet more appropriate.

Next let us discuss whether or not the keto–keto configuration, i.e., double PT is plausible. There is experimental evidence that this configuration is not accessible for electronically excited BBXHQ: methylation of one OH group did not alter the emission spectrum in *n*-heptane at room temperature [24]. Also the keto–keto form can not be represented by a single valence-bond electron pairing scheme and thus has chemical intuition against it. Yet this tautomer was involved in our explanations of the rich vibronic line spectrum up to now. We tried instead to simulate the vibronic spectrum with only the other three tautomers in the excited electronic state. In this case one needs a large and complex residual coupling W to produce the triplet vibronic structure (i.e., to give all three eigenstates sufficient oscillator strength). This large coupling however implies that more proton vibrational states are required for a converged calculation, thereby introducing nondiagonal coupling in the space of proton excitations which in turn destroys the regular triplet pattern. We conclude that within the four-mode model, all four excited isoenergetic tautomers are needed to simulate the vibronic spectrum – the doubly proton-transferred keto–keto form should exist in S_1.

To examine this hypothesis, quantum-chemical calculations were performed for the enol–enol ground state and for the first excited state in the enol–enol, enol–keto, and keto–keto geometry. The semiempirical electronic Hamiltonians AM1 [31], PM3 [32], and SAM1 [33] were used with the program package AMPAC 6.55 [30]. Calculations employed complete active space configuration interaction ($CI = 12$–18) and the geometries were optimized with and without symmetry constraints. All three methods predict the same ordering of excited state conformations: the highest is enol–enol , keto–keto is found close to it or just below within a typical error band of $\pm 600\ cm^{-1}$, and lowest is the enol–keto conformation. We find that for $CI \geqslant 16$, PM3 converges best and also predicts electronic transition frequencies closest to experiment. The same energy differences between the excited conformations are found with AM1 while SAM1 produces larger differences. Values for the potential energy (calculated with PM3 and $CI = 18$) of stable forms in the excited state, relative to the enol–enol ground state, are given in Fig. 1. With regard to absolute values, note that the calculated vertical excitation or emission frequencies for the enol–enol form are off by about $2500\ cm^{-1}$ from experiment. On the other hand, the relative energetic order of the S_1 tautomers is probably accurate only to $\pm 600\ cm^{-1}$ as noted above. The most important result for this study is that a keto–keto tautomer is predicted at the same energy as the originally excited enol–enol form in S_1. This finding supports our interpretation of the vibronic line spectrum in Fig. 3.

Having all parameters for our model available we shall now study the dynamics. The wavepacket motion (double proton coordinate probability distribution, Eq. (5)) as inferred from the frequency-domain spectrum is shown in Fig. 4. In a weakly polar solvent, PT in BBXHQ has a time constant of 110 fs: the reaction occurs during the first half-cycle of the active skeletal vibration. In the gas phase the polar enol–keto tautomers are no longer stabilized by the solvent. As a consequence, no substantial probability redistribution from the enol configuration to the enol–keto configurations ($|\psi_{A\mu=0}\psi_{B\mu=0}\Phi_{AB}\rangle$, or $|\psi_{B\mu=0}\psi_{A\mu=0}\Phi_{BA}\rangle$) appears at this short time.

In conclusion, single and double PT in the excited state of a large molecule, BBXHQ, was treated in the frame of dissipative quantum dynamics. Vibronic spectra and femtosecond wavepacket evolution are approached in a unified way, including energy redistribution. A model Hamiltonian was developed which treats the motion of two protons, each coupled indirectly to the skeletal vibration of nearby heteroatoms, in the adiabatic approximation. Application to a rich vibronic line spectrum suggested the existence of a keto–keto tautomer in excited BBXHQ. This was confirmed by quantum-chemical calculations.

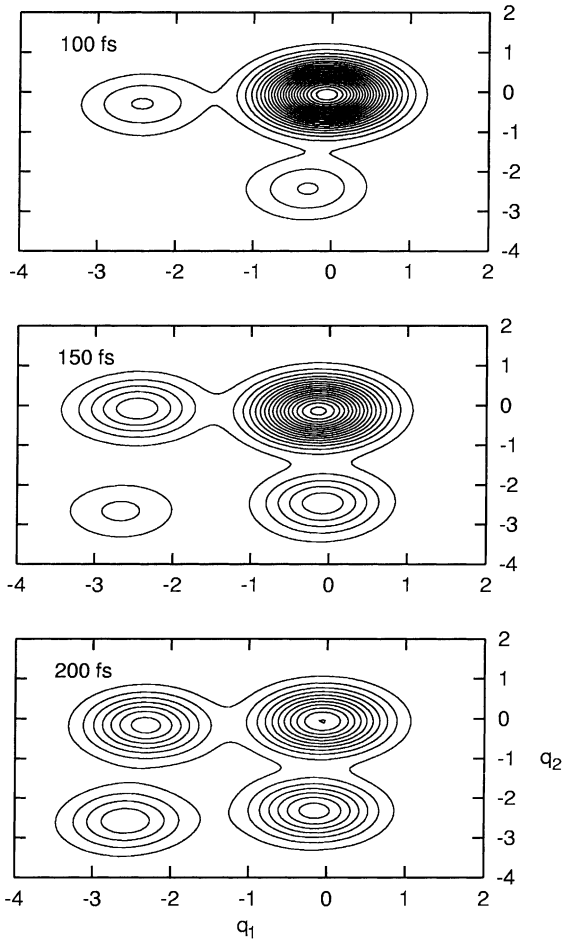

Fig. 4. Wavepacket dynamics of the double-proton motion with parameters equal to those used for the spectrum in Fig. 3. The dimensionless coordinates q_1 and q_2 are defined as given in the caption of Table 1.

Acknowledgements

We gratefully acknowledge financial support by the Deutsche Forschungsgemeinschaft through Sonderforschungsbereich 450.

Note added in Proof

Ab-initio calculations with multi-reference second-order Møller Plesset perturbation theory [S. Grimme, M. Waletzky, Phys. Chem. Chem. Phys. 2 (2000) 2075] confirm the ordering of states obtained here with semiempirical methods and are in very good agreement with stationary and excited state optical spectra.

References

[1] C.L. Perrin, J.B. Nielsen, Annu. Rev. Phys. Chem. 48 (1997) 511.
[2] J.D. Watson, F.H.C. Crick, Nature 171 (1953) 946.
[3] J. Manz, L. Wöste (Eds.), Femtosecond Chemistry, Verlag Chemie, Weinheim, 1995.
[4] A. Douhal, F. Lahmani, A.H. Zewail, Chem. Phys. 207 (1996) 477.
[5] S. Steenken, Biol. Chem. 378 (1997) 1293.
[6] J. Catalan, M. Kasha, J. Phys. Chem. A 104 (2000) 10812.
[7] A. Douhal, S.K. Kim, A.H. Zewail, Nature 378 (1995) 260.
[8] A. Douhal, V. Guallar, M. Moreno, J.M. Lluch, Chem. Phys. Lett. 256 (1996) 370.
[9] T. Fiebig, M. Chachisvilis, M. Manger, A.H. Zewail, A. Douhal, I. Garcia-Ochoa, A. de La Hoz Ayuso, J. Phys. Chem. A 103 (1999) 7419.
[10] S. Takeuchi, T. Tahara, J. Phys. Chem. A 102 (1998) 7740.
[11] C. Chudoba, E. Riedle, M. Pfeiffer, T. Elsässer, Chem. Phys. Lett. 263 (1996) 622.
[12] S. Lochbrunner, A.J. Wurzer, E. Riedle, J. Chem. Phys. 112 (2000) 10699.
[13] N.P. Ernsting, S.A. Kovalenko, T. Senyushkina, J. Saam, V. Farztdinov, J. Phys. Chem. 105 (2001) 3443.
[14] K. Fuke, K.J. Kaya, J. Phys. Chem. 93 (1989) 614.
[15] N.P. Ernsting, J. Phys. Chem. 89 (1985) 4932.
[16] M. Pfeiffer, A. Lau, K. Lenz, T. Elsaesser, Chem. Phys. Lett. 268 (1997) 258.
[17] D. Borgis, J.T. Hynes, J. Phys. Chem. 100 (1996) 1118.
[18] P. Blaise, O. Henri-Rousseau, Chem. Phys. 256 (2000) 85.
[19] V. May, O. Kühn, Charge and Energy Transfer Dynamics in Molecular Systems, Wiley-VCH, Weinheim, 1999.
[20] V. Gualla, V.S. Batista, W.H. Miller, J. Chem. Phys. 110 (1999) 9922.
[21] A.A. Stöckli, B.H. Meier, R. Kreis, R. Meyer, R.R. Ernst, J. Chem. Phys. 93 (1990) 1502B.
[22] J.-Y. Fang, S. Hammes-Schiffer, J. Chem. Phys. 107 (1997) 8933.
[23] S. Mukamel, Principles of Nonlinear Optical Spectroscopy, Oxford University Press, New York, 1995.
[24] A. Mordzinski, A. Grabowska, W. Kuhnle, A. Krowczyski, Chem. Phys. Lett. 101 (1983) 291.
[25] A. Mühlpfordt, U. Even, N.P. Ernsting, Chem. Phys. Lett. 263 (1996) 178.
[26] J.J. Dannenberg, J. Mol. Struct. (Theochem.) 401 (1997) 279.
[27] F. Neugebauer, V. May, Chem. Phys. Lett. 289 (1998) 67.
[28] A. Mühlpfordt, Thesis, Humboldt-Universität zu, Berlin, 1998.
[29] Th. Arthen-Engeland, T. Bultmann, N.P. Ernsting, M.A. Rodriguez, W. Thiel, Chem. Phys. 163 (1992) 43.
[30] AMPAC 6.55. 1999, Semichem, Inc. PO Box 1649 Shawnee KS 66222.
[31] M.J.S. Dewar, E.G. Zoebisch, E.F. Healy, J.J.P. Stewart, J. Am. Chem. Soc. 107 (1985) 3902.
[32] J.J.P. Stewart, J. Comput. Chem. 10 (1989) 209,221.
[33] M.J.S. Dewar, C. Jie, J. Yu, Tetrahedron 49 (1993) 5003.